DEND Mutation in Kir6.2 (*KCNJ11*) Reveals a Flexible N-Terminal Region Critical for ATP-Sensing of the K_{ATP} Channel

Joseph C. Koster, Harley T. Kurata, Decha Enkvetchakul, and Colin G. Nichols
Department of Cell Biology and Physiology, Washington University School of Medicine, St. Louis, Missouri 63110

ABSTRACT ATP-sensitive K^+-channels link metabolism and excitability in neurons, myocytes, and pancreatic islets. Mutations in the pore-forming subunit (Kir6.2; *KCNJ11*) cause neonatal diabetes, developmental delay, and epilepsy by decreasing sensitivity to ATP inhibition and suppressing electrical activity. Mutations of residue G53 underlie both mild (G53R,S) and severe (G53D) forms of the disease. All examined substitutions (G53D,R,S,A,C,F) reduced ATP-sensitivity, indicating an intolerance of any amino acid other than glycine. Surprisingly, each mutation reduces ATP affinity, rather than intrinsic gating, although structural modeling places G53 at a significant distance from the ATP-binding pocket. We propose that glycine is required in this location for flexibility of the distal N-terminus, and for an induced fit of ATP at the binding site. Consistent with this hypothesis, glycine substitution of the adjacent residue (Q52G) partially rescues ATP affinity of reconstituted Q52G/G53D channels. The results reveal an important feature of the noncanonical ATP-sensing mechanism of K_{ATP} channels.

INTRODUCTION

The ATP-sensitive K^+-channel (K_{ATP}) controls cellular function in neurons, β-cells, and other tissues by translating changes in cellular metabolism (represented by the [ATP]/[ADP] ratio) into changes in electrical activity. Aberrantly elevated K_{ATP} activity is predicted to decrease excitability, and thereby compromise cell function. An increase in K_{ATP} activity in the pancreatic β-cell impairs insulin release at stimulatory blood-glucose concentrations (1–3). In addition, channel overactivity in the central nervous system is predicted to underlie seizure events (4–7), and it appears that ketogenic diets may actually protect against seizure by enhancing the damping effect of K_{ATP} channels on electrical activity (8). Activating mutations in K_{ATP} (both the Kir6.2 (*KCNJ11*) and SUR1 (*ABCC8*) subunits) represent a common cause of neonatal diabetes mellitus (NDM) in humans, a disease characterized as an insulin-dependent hyperglycemia diagnosed before 6 months of age (9). The diabetes may be either permanent (PNDM) or transient (TNDM) in form (10,11). In the most severe cases, K_{ATP} mutations are associated with neurological features that include developmental delay (both motor and intellectual), epilepsy, and neonatal diabetes (referred to as DEND syndrome) (12), and these extrapancreatic symptoms likely reflect K_{ATP} overactivity in muscle, peripheral neurons, and/or brain. Importantly, sulfonylureas, which specifically block the K_{ATP} channel, can reverse the diabetes and ameliorate the associated neurological features (6,13,14).

Structurally, the K_{ATP} channel is a hetero-octomer comprised of four pore-forming Kir6.2 subunits bordered by four regulatory SUR1 subunits. Whereas SUR1 confers sensitivity of the channel to stimulatory MgADP and the inhibitory sulfonylureas, the Kir6.2 subunit confers the characteristic ATP-inhibition of the channel. The predicted ATP-binding pocket in Kir6.2 is formed by residues located in both the cytoplasmic N- and C-termini such that each Kir6.2 subunit in the tetramer is capable of binding a molecule of ATP, and binding of ATP to one subunit is sufficient to cause channel closure (15,16).

To date, more than 40 heterozygous activating mutations in Kir6.2 (*KCNJ11*) have been reported worldwide and shown to be variably associated with both the transient and permanent forms of the disease (17–19). Without exception, these diabetes-causing mutations activate K_{ATP} by increasing the half-inhibitory ATP concentration ($K_{1/2,ATP}$) (20–24). Mechanistically, these mutations decrease ATP-sensitivity either 1), by directly decreasing ATP-binding to Kir6.2 (e.g., R50P), or 2), by altering intrinsic channel-gating (i.e., increasing open probability in the absence of ATP ($p_{o,zero}$), e.g., Q52R). In the latter case, ATP-sensitivity is reduced allosterically, because ATP predominantly interacts with closed states of the channel, to which access is reduced when the open state is favored (25,26).

Recently we described the phenotype and therapy of an adult patient with intermediate DEND (developmental delay and neonatal diabetes, but not epilepsy) attributable to the G53D mutation in *KCNJ11* (14). Functional analysis of reconstituted G53D channels (Kir6.2[G53D] + SUR1) demonstrated a significant rightward shift in the ATP dose-response curve. Consistent with channel overactivity in the cellular environment, whole-cell K_{ATP} currents were significantly increased in transfected mammalian cells expressing G53D channels, compared with the wild-type (WT) (14). Here, we characterize the effects of mutations in this region in greater detail. Although G53 resides outside the predicted

Submitted June 5, 2008, and accepted for publication August 6, 2008.

Address reprint requests to Joseph C. Koster or Colin G. Nichols, Dept. of Cell Biology and Physiology, Washington University School of Medicine, 660 South Euclid Ave., St. Louis, MO 63110. E-mail: jkoster@cellbiology.wustl.edu or cnichols@wustl.edu.

Editor: Dorothy A Hanck.

0006-3495/08/11/4689/09 $2.00

doi: 10.1529/biophysj.108.138685

ATP-binding pocket, the G53D mutation alters ATP-sensitivity without altering the intrinsic gating behavior of the channel (as reflected by the $p_{o,zero}$ and kinetic behavior of single channels). This contrasts sharply with all other reported non-ATP-binding mutations that indirectly alter ATP-sensitivity by changing gating kinetics (20,21,24). Furthermore, we show that the G53 position is highly intolerant of amino-acid substitutions with respect to ATP-sensitivity, but the loss of ATP-sensitivity can be partially rescued by glycine substitution at the adjacent residue (Q52G). These results demonstrate that flexibility of this N-terminus region is necessary for efficient ATP binding, and this leads us to speculate that the rotational flexibility of G53 constitutes an interfacial gating hinge, separate from the gate involved in ion conduction, which allows for movement of the N-terminal region and an induced fit of ATP at its binding pocket.

METHODS

Molecular biology

We cloned Kir6.2 into the *Eco*RI/*Cla*I sites of pCMV6b and the parental plasmid DNA was used to generate Kir6.2 mutations using the QuickChange Site Directed Mutagenesis Kit (Stratagene, La Jolla, CA). The SUR1 was cloned into the pECE expression vector. The nucleotide sequences of mutant Kir6.2 constructs were verified by fluorescence-based cycle sequencing, using AmpliTaq DNA polymerase, FS (Perkin-Elmer, Foster City, CA), and an ABI Prism DNA sequencer (Perkin-Elmer).

Expression of K_{ATP} channels in COSm6 cells

COSm6 cells were plated at a density of $\sim 2.5 \times 10^5$ cells per well (30-mm six-well dishes) and cultured in Dulbecco's modified Eagle's medium plus 10 mM glucose (DMEM-HG), supplemented with fetal calf serum (FCS, 10%). The COSm6 cells were transfected with cDNA using FuGENE 6 Transfection Reagent (Roche Diagnostics, Indianapolis, IN). Total DNA (0.3 μg Kir6.2 (27) plus 0.5 μg SUR1 (28) plus 0.3 μg green fluorescent protein as a marker for transfection) was mixed with FuGENE 6 and pre-incubated for 1 h. Cells were incubated in the presence of the transfection mixture for 12–24 h, and plated on sterile glass coverslips overnight before patch-clamp experiments.

Electrophysiological methods

Patch-clamp experiments were performed at room temperature in an oil-gate chamber that allowed the solution bathing the exposed surface of the isolated patch to be changed rapidly. The COSm6 cells that fluoresced green under ultraviolet illumination were selected for patch-clamping 3–5 days after transfection. Membrane patches were voltage-clamped using a CV-4 head stage, an Axopatch 1-D amplifier, a Digidata 1322A digitizer board (all from Axon Instruments, Union City, CA), and an MP-225 micromanipulator (Sutter Instrument, Novato, CA). All currents were measured at a membrane potential of -50 mV (pipette voltage, $+50$ mV). Data were collected using the pClamp 8.2 software suite (Axon Instruments) and Microsoft Excel (Microsoft, Redmond, WA). Bath and pipette control solutions (K_{INT}) contained 150 mM KCl, 10 mM HEPES, and 1 mM EGTA, pH 7.4. Where indicated, ATP was added to the bathing solution as dipotassium salts. Phosphotidyinositol-4,5-bisphosphate (PIP_2; Avanti Polar Lipids, Alabaster, AL) was dissolved in K_{INT} to a stock concentration of 1 mg/mL, and diluted to a working concentration of 5 μg/mL.

Data analysis

Quantitative analysis of ATP inhibition

The ATP dose-response was quantified by fitting the raw data with a Hill equation:

$$I_{rel} = 1/(1 + ([ATP]/K_{1/2,ATP})^H), \quad (1)$$

where I_{rel} is the current relative to that in the absence of ATP, [ATP] is the ATP concentration, $K_{1/2,ATP}$ is the half-maximal inhibitory ATP concentration, and H is the Hill coefficient, which was fixed at 1.3.

Single-channel analysis

Unconditional mean lifetimes in the open and closed states were determined from idealized (using pClamp 8.2 software) records of channel activity from patches containing 1–4 channels.

Estimation of $p_{o,zero}$

Two approaches were used to estimate $p_{o,zero}$, the initial open probability (in zero ATP), after the excision of isolated membrane patches containing multiple channels. In method I, PIP_2 was added to the patch until the current reached a saturating level (I_{PIP2}). This was assumed to represent a maximum $p_{o,zero}$ of $\sim$0.97 (26). The fold increase in current was calculated (fold increase $= I_{initial}/I_{PIP2}$; see Fig. 2), and $p_{o,zero}$ was estimated from:

$$p_{o,zero} = 0.97/(\text{fold increase}). \quad (2)$$

Method II involved noise analysis (NA). Mean $p_{o,zero}$ was estimated from stationary fluctuation analysis of macroscopic currents (29,30) on short ($<$1 s) recordings of currents in zero [ATP] and in 5 mM [ATP]. Currents (4 pA $<$ mean current $<$ 4 nA, at -50 mV, corresponding to $\sim$1–1000 channels) were filtered at 1 kHz and digitized at 3 kHz, with 12-bit resolution. Mean patch current (I) and variance (α^2) in the absence of ATP were obtained by subtraction of the mean current and variance in 5 mM ATP (i.e., assuming all channels were closed), respectively. Single-channel current (i) was assumed to be -3.75 pA, corresponding to a WT single-channel conductance of 75 pS. The $p_{o,zero}$ was then estimated according to

$$p_{o,zero} = 1 - (\alpha^2/[i \times I]). \quad (3)$$

Model simulation of $p_{o,zero}$ versus $K_{1/2,ATP}$ relationship

Although complex models of K_{ATP} gating can describe essentially all of the gating behavior of the channel (16,31,32), a simplified four-state model quantitatively describes channel behavior over a wide range of conditions, including changing levels of ATP and PIP_2, as well all mutational effects on ATP affinity (K_D) or the intrinsic open-closed equilibrium (K_{CO}) (model II of Enkvetchakul et al. (26)):

$$C \underset{ATP}{\overset{K_D}{\rightleftarrows}} C_{in} \overset{K_{CO}}{\rightleftarrows} O \rightleftarrows C_F.$$

In this kinetic scheme, C represents the ATP-dependent closed state, C_{in} the ATP-independent closed state, C_F the fast closed state, and O the open state. K_D is the dissociation constant for the ATP-binding step, and K_{CO} is the equilibrium constant for the open-to-closed (C_{in}) transition. The key feature of this model is that ATP acts by binding to a closed state and, in consequence, the apparent ATP-sensitivity can be reduced either by shifting the equilibrium between the C_{in} and O states toward the open state (increasing K_{CO}), or by reducing ATP-binding (increasing K_D). Model simulations were generated using Microsoft Excel.

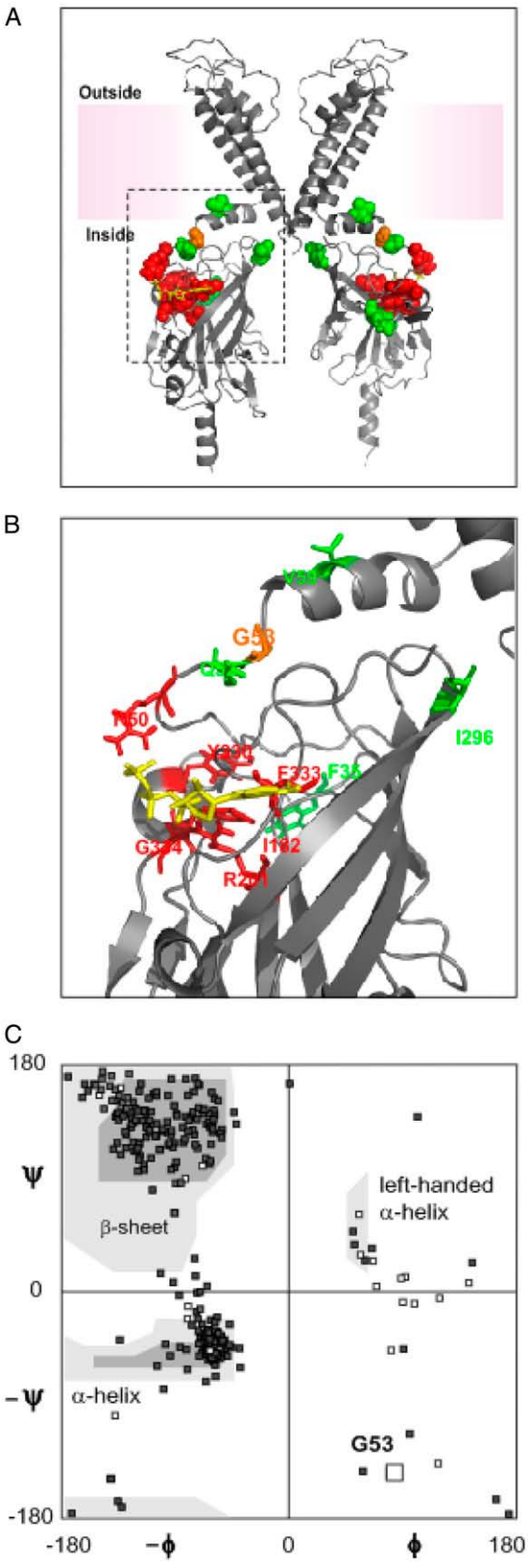

FIGURE 1 Location of G53 in predicted Kir6.2 structure. (*A*) Ribbon diagram of two of four Kir6.2 subunits that form K^+-selective pore in K_{ATP}. Dashed box corresponds to region that was magnified to create *B*. (*B*) Residues (*highlighted*) in Kir6.2 that are mutated in neonatal diabetes. Residues are classified as those that form part of the ATP-binding pocket (*red*), or are involved in channel-gating, and therefore indirectly in ATP-sensitivity (*green*). The G53 residue that neither forms part of the ATP-binding pocket nor alters gating behavior when mutated is shown in orange. The bound ATP molecule is shown in yellow, and the interfacial slide-helix region is shown as α-helical. (*C*) Conformational angles around α-carbons in amino-acid backbone of Kir6.2 are shown in a Ramachandran plot (ψ versus ϕ). Bond angles associated with α-helical and β-sheet structures are indicated. Glycine residues are shown as open symbols, and all other residues are shown as solid symbols. Ramachandran data analysis was performed using Visual Molecular Dynamics software (http://www.ks.uiuc.edu/Research/vmd/).

Calculations of free energy for ATP-binding

The free energy of ATP-binding was calculated for individual membrane patches using

$$\Delta G^\circ = -2.303\,RT\log_{10}[K_D], \tag{4}$$

where R is the gas constant (1.98×10^{-3} kcal mol^{-1}deg^{-1}), T is the absolute temperature (298 K), and K_D is the dissociation constant for ATP in the above model. For mutant K_{ATP} channels (G53D, Q52G, and G53D/Q52G), the free-energy effect of the mutation ($\Delta\Delta G$) was obtained by subtracting the averaged value of ΔG for wild-type channels (see Fig. 6 *F*).

RESULTS

Molecular model of Kir6.2 and location of G53

Structural modeling of the Kir6.2 tetrameric pore places the G53 residue distal to the ATP-binding pocket and adjacent to the slide helix, which previously has been implicated in Kir channel gating (Fig. 1, *A* and *B*) (15,33). Mutations of nearby residues Q52 and V59 (Q52R and V59M) also underlie NDM, and were shown to reduce ATP-sensitivity indirectly by increasing the open probability of the channel (20,21). Just distal to G53 in the primary sequence is residue R50, which forms part of the binding pocket and is predicted to interact electrostatically with the γ-phosphate of ATP. Consistent with this role, the diabetes-causing R50P mutation significantly reduces the ATP-sensing of reconstituted channels, but without altering intrinsic gating behavior (34).

Intolerance of K_{ATP} to amino-acid substitutions at the G53 residue

Coexpression of WT Kir6.2 and SUR1 in COSm6 cells generates K_{ATP} channels that are inhibited by ATP in excised patch-clamp experiments, with an ATP-sensitivity similar to that of native channels ($K_{1/2,ATP} = \sim 10\ \mu M$; Fig. 2) (27). Conversely, homomeric mutant channels containing substitutions at residue G53 (Kir6.2[G53x] + SUR1) all exhibit a significant decrease in ATP-sensitivity relative to WT: $K_{1/2,ATP} = 190\ \mu M$ (G53D), $124\ \mu M$ (G53F), $87\ \mu M$ (G53S), $66\ \mu M$ (G53A), $62\ \mu M$ (G53C), and $52\ \mu M$ (G53R). The G53R and G53S mutations underlie several cases of

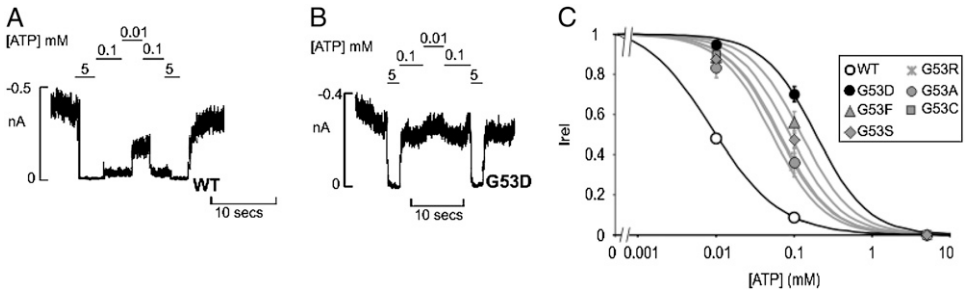

FIGURE 2 Reduced ATP-sensitivity of reconstituted K_{ATP} channels containing G53 mutant subunits. Representative currents were recorded from inside-out membrane patches from COS cells expressing (*A*) wild-type (Kir6.2(WT) + SUR1) or (*B*) mutant (Kir6.2(G53D) + SUR1) K_{ATP} channels at −50 mV in K_{int} solution (see Methods). Patches were exposed to differing [ATP], and baseline current was determined by exposure to ATP (5 mM). (*C*) Steady-state dependence of membrane current on [ATP] (relative to current in zero ATP (I_{rel})) for wild-type and G53X-containing channels. $K_{1/2,ATP}$ = 10 μM (WT), 190 μM (G53D), 124 μM (G53F), 87 μM (G53S), 66 μM (G53A), 62 μM (G53C), and 52 μM (G53R). Data points represent mean ± SE (n = 4–30 patches). Fitted lines correspond to least-squares fits of a Hill equation (see Methods).

TNDM, and functional analyses of these mutants expressed in *Xenopus* oocytes demonstrated similar shifts in ATP-sensitivities (23).

Unaltered open probability in G53 mutated channels

Two approaches were used to estimate open probability in the absence of inhibitory ATP ($p_{o,zero}$) in macroscopic recordings: nonstationary NA (method II) (29), and the application of PIP_2 (method I) (20)(see Methods). Both methods gave similar values for $p_{o,zero}$ for both WT and G53D mutant channels (Fig. 3; $p_{o,zero}$= 0.47 (WT) and 0.49 (G53D), averages from both methods I and II). Similarly, the TNDM-causing G53R mutation did not significantly affect $p_{o,zero}$ (0.57), although the G53S mutation did slightly increase open probability relative to WT ($p_{o,zero}$ = 0.67). This increase in $p_{o,zero}$ was statistically significant by the NA method, but did not reach significance using the PIP_2 method. By comparison, the diabetes-linked Glu to Arg mutation at the adjacent residue 52 (Q52R) significantly increased the open probability ($p_{o,zero}$ = ~0.9), and this gating effect can fully account for the reported decrease in ATP-sensitivity of Q52R channels (20,21).

Altered relationship between ATP-sensitivity and open probability in G53D channels

As described above, multiple studies of channel-gating demonstrated a nonlinear relationship between $p_{o,zero}$ and $K_{1/2,\ ATP}$ (26,35,36). Wild-type channels have an intrinsic p_o of ~0.5, and an intrinsic $K_{1/2,ATP}$ of ~10 μM (Fig. 4, *A* and *C*). Application of PIP_2 leads to a gradual increase in $p_{o,zero}$ and $K_{1/2,ATP}$, in accordance with the prediction of the model (*solid lines* in Fig. 4 *C* indicate the prediction of the inset model with parameters from model II of Enkvetchakul et al. (26), with K_D = 5.8 μM). The gating mutant Q52R has a much higher intrinsic $p_{o,zero}$ (~0.9) and $K_{1/2\ ATP}$ (~125 μM), reflecting a higher intrinsic K_{CO}, but the response to PIP_2 follows the same relationship, reflecting no change in ATP affinity (K_D). The model predicts that a Kir6.2 mutation that alters ATP binding alone will be shifted to a different relationship, with a higher $K_{1/2,ATP}$ for any given $p_{o,zero}$. This is the case for the G53D channels (Fig.4 *C*, *upper solid line*). At similar open probabilities, a higher $K_{1/2\ ATP}$ was measured for G53D channels compared with WT, corresponding to a K_D value of 72 μM (i.e., ~13-fold lower than WT). The finding that G53 mutations affect ATP affinity, but not intrinsic gating, is initially surprising, given that G53 is located outside the ATP-binding pocket (Fig. 1).

Unaltered gating behavior in G53D channels

To examine the gating kinetics of G53D channels in detail, single-channel currents were recorded from cells expressing WT or mutant K_{ATP} channels (Fig. 5). Consistent with the macroscopic analysis of channel open probability, there was no significant difference in $p_{o,zero}$ values between WT and

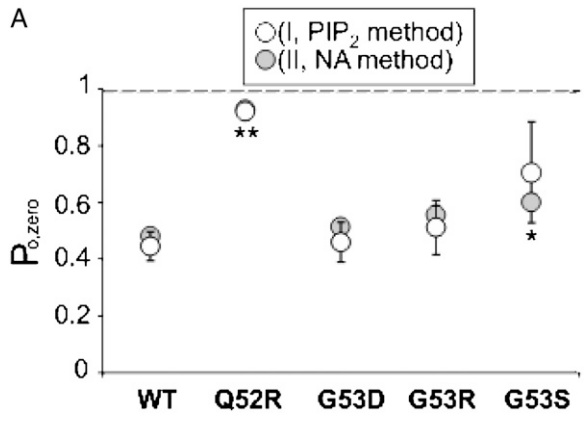

FIGURE 3 Unaltered maximum open probabilities of reconstituted K_{ATP} channels containing G53 mutations. Open probability in absence of ATP ($p_{o,zero}$) was calculated from individual membrane patches expressing reconstituted wild-type and G53x mutant channels. Method I used PIP_2 stimulation to estimate $p_{o,zero}$, and method II used nonstationary noise analysis (NA; see Methods). For comparison, the $p_{o,zero}$ of the gating mutation, Q52R, is also shown (20). Data points represent mean ± SE (n = 5–17 patches, method I; n = 10–27 patches, method II). *$p < 0.05$ and **$p <$ 0.01 compared with WT by unpaired Student's t-test.

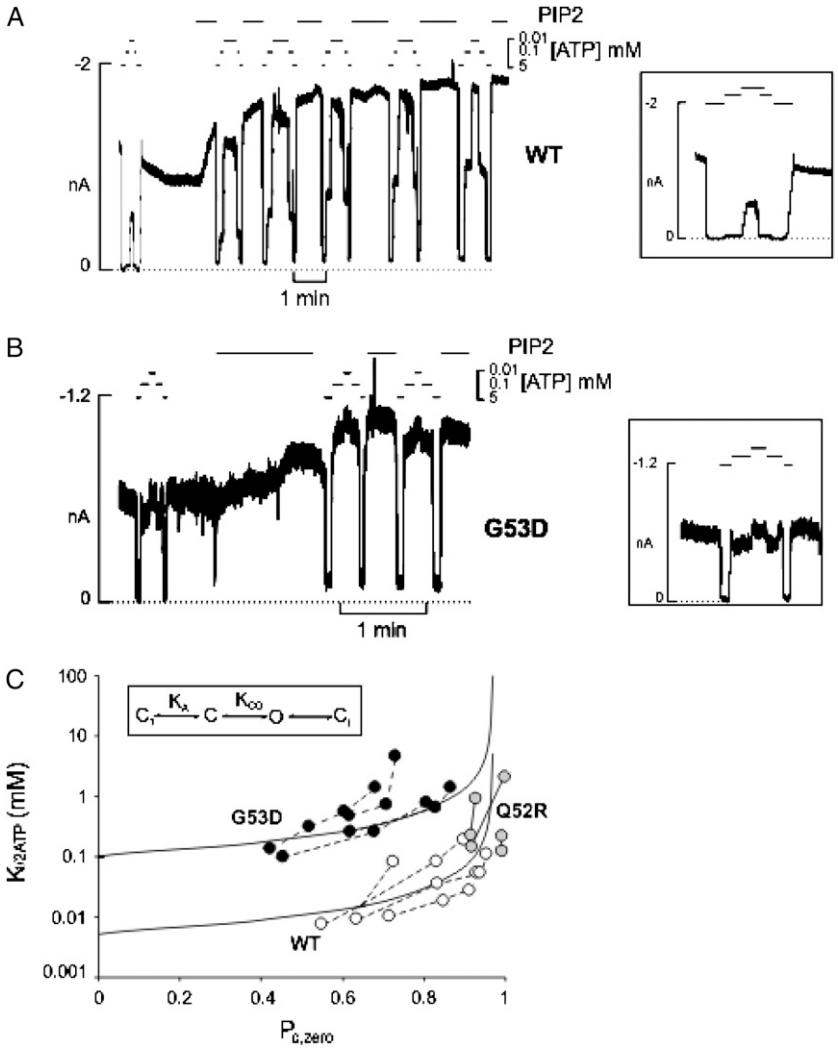

FIGURE 4 PIP_2 stimulation of wild-type and mutant (G53D) K_{ATP} channels. Representative currents were recorded from membrane patches containing either (*A*) wild-type (Kir6.2(WT) + SUR1) or (*B*) mutant (Kir6.2[G53D] + SUR1) K_{ATP} channels at −50 mV. Bars indicate application of PIP_2 (5μg/mL) or different [ATP] (as shown). Lower dashed line indicates zero current. *Insets*: Expanded records from first 50–100 s after patch excision, from which ATP-sensitivity and open probability (NA method) were estimated. (*C*) Relationship between $p_{o,zero}$ and $K_{1/2,\ ATP}$ (mM). Solid lines represent modeled data calculated from model II of Enkvetchakul et al. (26). Symbols represent data points calculated from individual membrane patches: WT (Kir6.2(WT) + SUR1), G53D (Kir6.2(G53D) + SUR1), or Q52R (Kir6.2(Q52R) + SUR1). Modeled data were fit using nonlinear regression analysis.

G53D single channels, although the estimated open probabilities were lower than those calculated using the indirect methods (Table 1). The gating behavior was also not different between WT and G53D channels with groups of openings being clustered in similarly timed bursts in both channels (Fig. 5), and both channels displayed similar mean open (τ_{open}) and closed times (τ_{closed}), as well as single-channel current (Table 1). By contrast the disease-causing Q52R mutation predictably displayed an increase in $p_{o,zero}$ in single channels with a significantly lower mean closed time (Fig. 5, Table 1). Together with the macroscopic analysis, these data strongly support the conclusion that gating behavior is not altered in G53D channels.

Ramachandran plot of Kir6.2

The intolerance for amino-acid substitutions at the G53 position with respect to ATP-sensitivity (Fig. 2) implies the importance of rotational flexibility at this position. The ϕ and ψ torsion angles around the α-carbons in the Kir6.2 model (15) were analyzed in a Ramachandran plot (37) (Fig. 1 *C*). Glycine has no side chain, and therefore can adopt ϕ and ψ angles in all four quadrants, and frequently occurs in regions of proteins where any other residue would be sterically hindered. Indeed, in the Ramachandran plot of the modeled Kir6.2 structure, the G53 residue is found in the lower right quadrant, occupied primarily by glycines and very few other amino acids (Fig. 1 *C*).

Importance of rotational flexibility at the G53 position for ATP-sensing of the channel

As detailed in the Discussion, we propose that residue G53 uniquely controls ATP-binding through a long-range action on the proximal N-terminus. Specifically, we suggest that G53 acts as a hinge to allow a rigid body movement of the distal N-terminus that is necessary to fully accommodate ATP at its binding pocket (38). The existence of a hinge

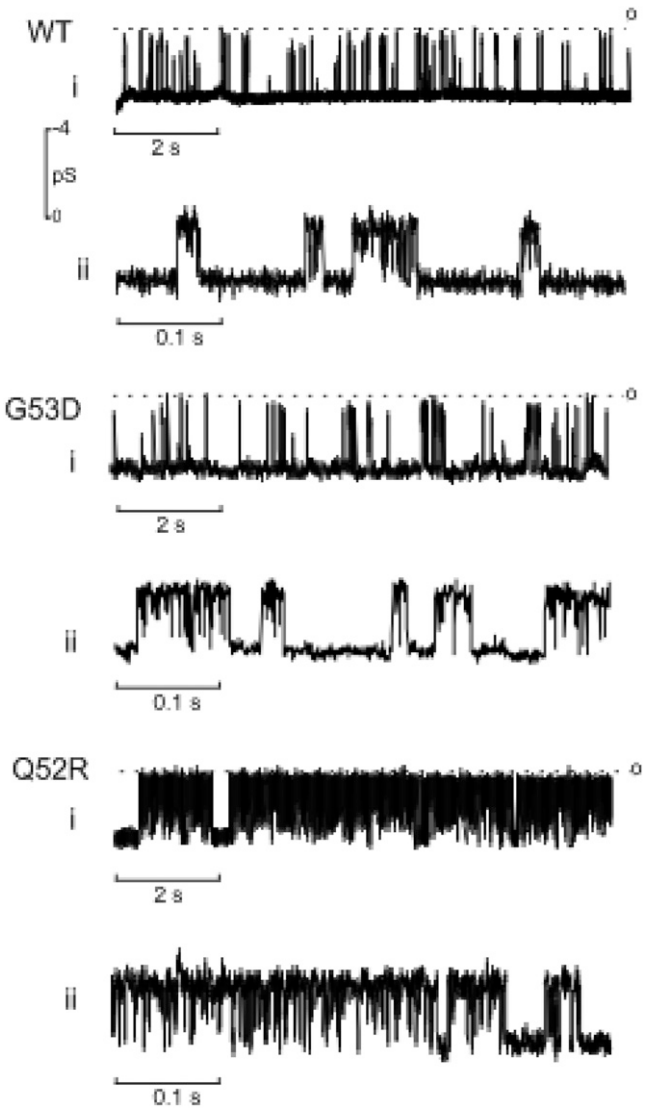

FIGURE 5 Unaltered gating behavior in single G53D channels. Representative single-channel currents were recorded at −50 mV from inside-out membrane patches excised from COS cells expressing either WT (Kir6.2 + SUR1), G53D (Kir6.2[G53D] + SUR1), or Q52R (Kir6.2[Q52R] + SUR1) channels. Two different timescales (2 s and 0.1 s) are shown for currents from each channel.

would explain the specific requirement for a glycine at this 53 position, but may also suggest that the hinge could be placed at an adjacent residue, to overcome the detrimental effect of substitutions at residue 53.

As shown in Fig. 6, *A–C*, the Q52G mutation (Kir6.2[Q52G] + SUR1) has no significant effect on ATP-sensitivity or on open probability, compared with the WT channel (Kir6.2WT] + SUR1). However, on the G53D background, the double-mutant channel (Kir6.2[Q52G,G53D] + SUR1) exhibits a significant *left* shift in ATP-sensitivity, compared with G53D channels alone ($K_{1/2,ATP}$ = 16.4 ± 1.7 μM (WT), 22.7 ± 3 μM (Q52G), 64.9 ± 6.1 μM (Q52G/G53D), and 226 ± 21.2 μM (G53D)). This shift in ATP-sensitivity corresponds to a considerably smaller increase in the free energy of ATP binding ($\Delta\Delta G = 0.99$ kcal mol^{-1}) for the combined mutant channel than is predicted from the additive effect of each mutant alone ($\Delta\Delta$G[Q52G] + $\Delta\Delta G$[Q52G/G53D] = 1.79 kcal mol^{-1}) (Fig. 6 *D*; see Methods). Although $p_{o,zero}$ is unaffected by either the Q52G or G53D single mutations, the Q52G/G53D double-mutant channel exhibits a small decrease in open probability that reached significance using the NA method (method II) (Fig. 6 *F*). Given the coupled relationship between $p_{o,zero}$ and $K_{1/2,ATP}$ (Fig. 4), the possibility exists that the decrease in ATP-sensitivity observed for the combined Q52G/G53D mutant channels is simply a consequence of the reduced open probability. However, when the $p_{o,zero}$ and $K_{1/2,ATP}$ relationship for the Q52G/G53D mutant is modeled as above (Fig. 4), the fit data reside on a different curve than that of the G53D channels alone (Fig. 6 *E*) (Kruskal-Wallis test, $p < 0.01$). This indicates that the decrease in open probability alone is insufficient to account for the observed shift in ATP-sensitivity of the double-mutant channel, and that Q52G can partly restore ATP affinity on the G53D background. Taken together, the data strongly implicate rotational flexibility in the immediate G53 region as necessary for high ATP affinity.

TABLE 1 Single-channel properties of wild-type and mutant Kir6.2 + SUR1 channels

Construct	*i* (nA)	τ_{open} (ms)	τ_{closed} (ms)	$p_{o,zero}$	*n*
WT	3.59 ± 0.2	3.5 ± 0.4	24.4 ± 5.4	0.145 ± 0.034	4
G53D	3.43 ± 0.1	3.4 ± 0.6	23.7 ± 8.1	0.198 ± 0.125	4
Q52R	3.58 ± 0.02	3.4 ± 0.5	0.9 ± 0.2*	0.796 ± 0.037*	3

i, single-channel current; τ_{open} and τ_{closed}, are unconditional mean open and closed times, determined from idealized records from *n* patches, each containing 1–4 active channels (mean number of channels per patch of 2.75, 2.5, and 1 for WT, G53D, and Q52R, respectively). $p_{o,zero} = \tau_{open}/(\tau_{open} + \tau_{closed})$.
*Significantly different from WT ($p < 0.001$).

DISCUSSION

K_{ATP} channel overactivity and disease severity

Previous studies demonstrated that distinct mutations of the G53 residue in Kir6.2 (G53S, G53R, and G53D) decrease ATP-sensitivity and underlie NDM or DEND (14,23). In the current study, a direct comparison indicates that the ATP-sensitivity of DEND-causing G53D channels is decreased ~20-fold, compared with a ~5–9-fold decrease for both the TNDM-associated G53S and G53R mutations. Because the relative ATP-sensitivity of the channel is an accurate predictor of K_{ATP} activity in vivo, these data are consistent with a genotype-phenotype relationship in which greater overactivity of K_{ATP} causes a more severe disease phenotype. Only with the most severe activating mutations (e.g., G53D) is overactivity associated with both diabetic and neurological symptoms, indicating that extrapancreatic tissues (e.g., muscle, nerve, and brain) are less sensitive to changes in

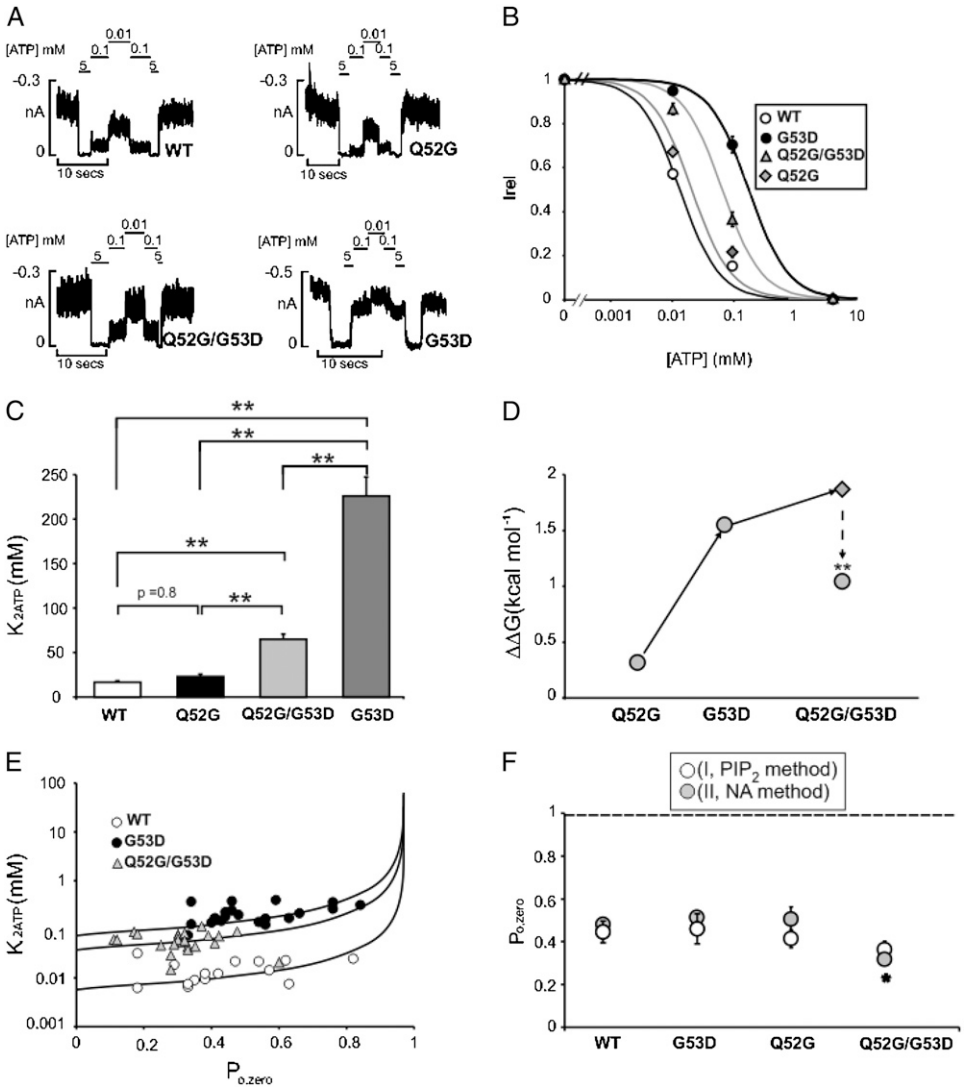

FIGURE 6 ATP affinity is partially restored in Q52G/G53D double-mutant channels. (*A*) Representative currents recorded from inside-out membrane patches from COS cells expressing WT, G53D, Q52G, or Q52G/G53D channels. Patches were exposed to various [ATP], as indicated. (*B*) Steady-state dependence of membrane current on [ATP] (relative to current in zero ATP (I_{rel})) for wild-type and G53x mutant channels. Data points represent mean ± SE ($n = 10$–30 patches). Fitted lines correspond to least-squares fits of a Hill equation (see Methods). (*C*) Average of $K_{1/2,ATP}$ values from individual patches, calculated using Hill equation: $^{**}p < 0.01$ by unpaired Student's *t*-test. (*F*) Maximum open probability in absence of ATP ($p_{o,zero}$) was calculated from individual membrane patches, as in Fig. 3. Data points represent mean ± SE ($n = 9$–17 patches, method I; $n = 9$–24 patches, method II). $^{*}p < 0.05$ by unpaired Student's *t*-test, compared with WT and G53D channels. (*E*) Relationship between $p_{o,zero}$ and $K_{1/2,ATP}$ (mM). Solid lines represent modeled data calculated from model II of Enkvetchakul et al. (26). Symbols represent data points calculated from individual membrane patches. Modeled data were fit using nonlinear regression analysis. For statistical analysis, the Kruskal-Wallis test was performed on equilibrium constants for ATP-binding (K_D derived from model fits, Eq. 3) from individual patches shown: Q52G/G53D versus G53D, $p < 0.01$; WT versus Q52G/G53D, $p < 0.001$; and WT versus G53D, $p < 0.001$. (*D*) Free energy of ATP binding for mutant K_{ATP} channels. The Gibbs free energy (ΔG(kJ mole^{-1})) was calculated from Eq. 3 for individual patches, using the fitted dissociation constant (K_D) (see Methods). To calculate $\Delta\Delta G$ (kcal mole^{-1}) values for mutant channels, the averaged free energy value from WT channels was subtracted from the averaged values for mutant K_{ATP} channels. Diamonds represent predicted $\Delta\Delta G$ (kcal mole^{-1}) value for combined mutant channel ($\Delta\Delta G$[G53D] + $\Delta\Delta G$[G53D/Q52G]), assuming an additive effect. Data points represent mean ± SE ($n = 9$–37 patches).

K_{ATP} activity than the pancreatic β-cell, and that a threshold of channel overactivity must be reached before neurological features become evident.

Mechanistic basis of G53D-associated diabetes

Homology modeling and ligand-docking analyses of Kir6.2 led to a detailed structural view of the ATP-binding site formed by residues in the N-termini and C-termini of Kir6.2 (Fig. 1) (15). In support of the model, residues that comprise the ATP-binding pocket decrease ATP-sensitivity when mutated, but without altering open probability. Consistently, residues located in regions outside the ATP-binding pocket decrease ATP-sensitivity when mutated, but do so indirectly through an increase in $p_{o,zero}$. The G53 residue is located at the N-terminal end of the slide helix of Kir6.2, and at a predicted distance of ~13 Å from the bound molecule of ATP (Fig. 1). Immediately adjacent to G53 in the primary structure (and located between G53 and the bound ATP molecule) is Q52, which when mutated to arginine also causes NDM (Q52R) (13). However, in this case, the Q52R mutation clearly reduces ATP-sensitivity indirectly through an increase in the intrinsic open probability (20). Both non-stationary NA and PIP_2 estimates demonstrate that $p_{o,zero}$ does not differ significantly between WT and G53 channels. Thus, the effect of the G53D mutation on ATP-sensitivity is clearly on ATP affinity, yet the residue is not physically part of the ATP binding site.

Recent molecular modeling, together with functional studies, supports a putative structure of the PIP_2 binding site

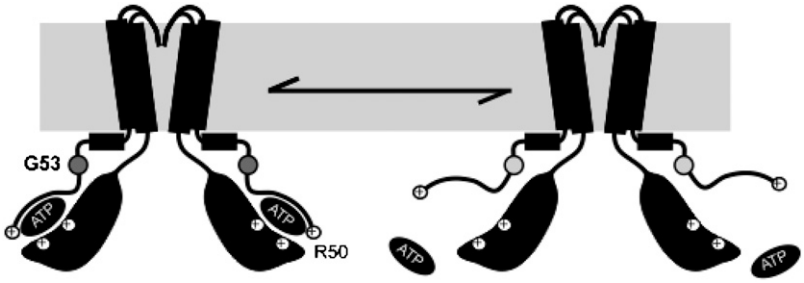

FIGURE 7 Proposed model for role of rotational flexibility at G53 position in control of ATP binding. Proposed movement of G53 residue that regulates ATP-binding is depicted. Simulations suggest that R50 resides in a region that forms a ''gate'' to the binding pocket (34,38). Reversible interaction of the channel with PIP_2 regulates movement of the gate, and therefore ATP-affinity. Residue G53 is hypothesized to represent a flexible ''gating hinge'' or, at the very least, a critical, flexible region necessary for high-affinity ATP-binding. Introduction of side chains at this position is predicted to alter ATP-binding efficacy.

on Kir6.2 that includes several residues in the slide helix region of the protein (38–41). Of these, R54 is predicted to interact electrostatically with the negative charges of the anionic headgroup of PIP_2. Therefore, given the close proximity of the slide helix region to the PIP_2 binding site, mutating Q52 to a positively charged arginine might electrostatically increase the binding affinity of PIP_2, which could then underlie the observed increase in $p_{o,zero}$, and the concurrent decrease in ATP-sensitivity of the reconstituted channel. Consistent with this interpretation, replacing Q52 with an uncharged glycine residue is not predicted to alter PIP_2 binding, explaining the lack of effect of the Q52G mutation itself on channel activity (Fig. 5).

Residue G53 as an interfacial gating hinge

Several lines of evidence support a requirement for rotational flexibility at residue G53 for normal ATP-sensing. First, all amino-acid substitutions at G53 were poorly tolerated with respect to ATP-sensitivity, including alanine, which has the second simplest side chain ($-CH_3$). Second, the Ramachandran plot of the Kir6.2 structural model reveals torsion angles around the α-carbon of G53 that are not found in most other amino acids in the structure. Third, introducing Q52G on the G53D background, which is expected to restore flexibility of the region, results in a decrease in free energy of ATP-binding, reflected in a leftward shift in the ATP-dose response curve. Although the Q52G/G53D double mutation decreases the open probability of reconstituted channels, this alone cannot fully account for the observed decrease in $K_{1/2,ATP}$ (Fig. 6).

Because the G53D mutation does not alter channel-gating, a logical interpretation of this data is that rotational flexibility is required for 1), directly regulating access of ATP to its binding pocket, 2), supporting a proper fit after ATP is bound, or 3), transducing the signal of ATP-binding to channel closure. Modeled simulations of PIP_2 binding to Kir6.2 demonstrate that the ATP-binding residue, R50, resides in a flexible loop that acts as a ''gate'' for ATP-binding (38). In the closed, locked position, R50 interacts electrostatically with the γ-phosphate of the bound ATP molecule. However, with PIP_2 stimulation, this flexible region moves, breaking the electrostatic interaction between the R50 residue and ATP, and carrying R50 away from the binding pocket, thereby decreasing ATP-binding affinity. Given the close connection of G53 to R50, and the observation that rotational flexibility is important at the G53 position, we speculate that G53 may act as ''gating hinge'', separate from the gate to ion conductance, necessary for flexibility of the proximal N-terminal region containing R50 (Fig. 7). Thus, any mutations in G53 that restrict movement of the ''hinge'' would decrease ATP-affinity. The existence of a glycine ''hinge'' will, of course, require detailed structural information that is not available in the current data set, in which we examined only the functional consequences of G53 mutations. Nevertheless, it is interesting that the glycine at position 53 is also found in the Kir6.1 channel, but is poorly conserved among other Kir channels (42). This may not be unexpected, insofar as Kir6.1 and Kir6.2 channels are the only members of the Kir family that are regulated by nucleotide-binding directly to the Kir subunit (43).

We are grateful to Drs. M. Sansom and F.M. Ashcroft for the Kir6.2 homology model.

This work was supported by National Institutes of Health grant DK69445 (to C.G.N.). We are also grateful to Diabetes Research and Training Grant DK-20579 (National Institutes of Health) for reagent support.

REFERENCES

1. Koster, J. C., B. A. Marshall, N. Ensor, J. A. Corbett, and C. G. Nichols. 2000. Targeted overactivity of beta cell K(ATP) channels induces profound neonatal diabetes. *Cell.* 100:645–654.
2. Koster, J. C., M. S. Remedi, R. Masia, B. L. Patton, A. Tong, and C. G. Nichols. 2006. Expression of ATP-insensitive KATP channels in pancreatic β-cells underlies a spectrum of diabetic phenotypes. *Diabetes.* 55:2957–2964.
3. Tarasov, A. I., H. J. Welters, S. Senkel, G. U. Ryffel, A. T. Hattersley, N. G. Morgan, and F. M. Ashcroft. 2006. A Kir6.2 mutation causing neonatal diabetes impairs electrical activity and insulin secretion from INS-1 beta-cells. *Diabetes.* 55:3075–3082.
4. Mlynarski, W., A. I. Tarasov, A. Gach, C. A. Girard, I. Pietrzak, L. Zubcevic, J. Kusmierek, T. Klupa, M. T. Malecki, and F. M. Ashcroft. 2007. Sulfonylurea improves CNS function in a case of intermediate DEND syndrome caused by a mutation in KCNJ11. *Nat. Clin. Pract. Neurol.* 3:640–645.
5. Bahi-Buisson, N., M. Eisermann, S. Nivot, C. Bellanne-Chantelot, O. Dulac, N. Bach, P. Plouin, C. Chiron, and P. de Lonlay. 2007. Infantile spasms as an epileptic feature of DEND syndrome associated with an activating mutation in the potassium adenosine triphosphate (ATP) channel, Kir6.2. *J. Child Neurol.* 22:1147–1150.
6. Shimomura, K., F. Horster, H. D. Wet, S. E. Flanagan, S. Ellard, A. T. Hattersley, N. I. Wolf, F. Ashcroft, and F. Ebinger. 2007. A novel mutation causing DEND syndrome. *Neurology.* 69:1342–1349.

7. Yamada, K., J. J. Ji, H. Yuan, T. Miki, S. Sato, N. Horimoto, T. Shimizu, S. Seino, and N. Inagaki. 2001. Protective role of ATP-sensitive potassium channels in hypoxia-induced generalized seizure. *Science*. 292:1543–1546.
8. Ma, W., J. Berg, and G. Yellen. 2007. Ketogenic diet metabolites reduce firing in central neurons by opening K(ATP) channels. *J. Neurosci*. 27:3618–3625.
9. Gloyn, A. L., E. R. Pearson, J. F. Antcliff, P. Proks, G. J. Bruining, A. S. Slingerland, N. Howard, S. Srinivasan, J. M. Silva, J. Molnes, E. L. Edghill, T. M. Frayling, I. K. Temple, D. Mackay, J. P. Shield, Z. Sumnik, A. van Rhijn, J. K. Wales, P. Clark, S. Gorman, J. Aisenberg, S. Ellard, P. R. Njolstad, F. M. Ashcroft, and A. T. Hattersley. 2004. Activating mutations in the gene encoding the ATP-sensitive potassium-channel subunit Kir6.2 and permanent neonatal diabetes. *N. Engl. J. Med*. 350:1838–1849.
10. Koster, J. C., A. Permutt, and C. G. Nichols. 2005. Diabetes and insulin secretion: the KATP connection. *Diabetes*. 54:3065–3072.
11. Hattersley, A. T., and F. M. Ashcroft. 2005. Activating mutations in Kir6.2 and neonatal diabetes: new clinical syndromes, new scientific insights, and new therapy. *Diabetes*. 54:2503–2513.
12. Slingerland, A. S., and A. T. Hattersley. 2005. Mutations in the Kir6.2 subunit of the KATP channel and permanent neonatal diabetes: new insights and new treatment. *Ann. Med*. 37:186–195.
13. Pearson, E. R., I. Flechtner, P. R. Njolstad, M. T. Malecki, S. E. Flanagan, B. Larkin, F. M. Ashcroft, I. Klimes, E. Codner, V. Iotova, A. S. Slingerland, J. Shield, J. J. Robert, J. J. Holst, P. M. Clark, S. Ellard, O. Sovik, M. Polak, and A. T. Hattersley. 2006. Switching from insulin to oral sulfonylureas in patients with diabetes due to Kir6.2 mutations. *N. Engl. J. Med*. 355:467–477.
14. Koster, J. C., F. Cadario, C. Peruzzi, C. Colombo, C. G. Nichols, and F. Barbetti. 2007. The G53D mutation in Kir6.2 (KCNJ11) is associated with neonatal diabetes and motor dysfunction in adulthood that is improved with sulfonylurea therapy. *J. Clin. Endocrinol. Metab*. 93:1054–1061.
15. Antcliff, J. F., S. Haider, P. Proks, M. S. Sansom, and F. M. Ashcroft. 2005. Functional analysis of a structural model of the ATP-binding site of the KATP channel Kir6.2 subunit. *EMBO J*. 24:229–239.
16. Enkvetchakul, D., and C. G. Nichols. 2003. Gating mechanism of KATP channels: function fits form. *J. Gen. Physiol*. 122:471–480.
17. Flanagan, S. E., E. L. Edghill, A. L. Gloyn, S. Ellard, and A. T. Hattersley. 2006. Mutations in KCNJ11, which encodes Kir6.2, are a common cause of diabetes diagnosed in the first 6 months of life, with the phenotype determined by genotype. *Diabetologia*. 49:1190–1197.
18. Vaxillaire, M., C. Populaire, K. Busiah, H. Cave, A. L. Gloyn, A. T. Hattersley, P. Czernichow, P. Froguel, and M. Polak. 2004. Kir6.2 mutations are a common cause of permanent neonatal diabetes in a large cohort of French patients. *Diabetes*. 53:2719–2722.
19. Massa, O., D. Iafusco, E. D'Amato, A. L. Gloyn, A. T. Hattersley, B. Pasquino, G. Tonini, F. Dammacco, G. Zanette, F. Meschi, O. Porzio, G. Bottazzo, A. Crino, R. Lorini, F. Cerutti, M. Vanelli, and F. Barbetti. 2005. KCNJ11 activating mutations in Italian patients with permanent neonatal diabetes. *Hum. Mutat*. 25:22–27.
20. Koster, J. C., M. S. Remedi, C. Dao, and C. G. Nichols. 2005. ATP and sulfonylurea sensitivity of mutant ATP-sensitive K^+ channels in neonatal diabetes: implications for pharmacogenomic therapy. *Diabetes*. 54:2645–2654.
21. Proks, P., J. F. Antcliff, J. Lippiat, A. L. Gloyn, A. T. Hattersley, and F. M. Ashcroft. 2004. Molecular basis of Kir6.2 mutations associated with neonatal diabetes plus neurological features. *Proc. Natl. Acad. Sci. USA*. 101:17539–17544.
22. Proks, P., C. Girard, and F. M. Ashcroft. 2005. Functional effects of KCNJ11 mutations causing neonatal diabetes: enhanced activation by MgATP. *Hum. Mol. Genet*. 14:2717–2726.
23. Gloyn, A. L., F. Reimann, C. Girard, E. L. Edghill, P. Proks, E. R. Pearson, I. K. Temple, D. J. Mackay, J. P. Shield, D. Freedenberg, K. Noyes, S. Ellard, F. M. Ashcroft, F. M. Gribble, and A. T. Hattersley. 2005. Relapsing diabetes can result from moderately activating mutations in KCNJ11. *Hum. Mol. Genet*. 14:925–934.
24. Girard, C. A., K. Shimomura, P. Proks, N. Absalom, L. Castano, D. N. Perez, and F. M. Ashcroft. 2006. Functional analysis of six Kir6.2 (KCNJ11) mutations causing neonatal diabetes. *Pflugers Arch*. 453:323–332.
25. Shyng, S., T. Ferrigni, and C. G. Nichols. 1997. Control of rectification and gating of cloned KATP channels by the Kir6.2 subunit. *J. Gen. Physiol*. 110:141–153.
26. Enkvetchakul, D., G. Loussouarn, E. Makhina, S. L. Shyng, and C. G. Nichols. 2000. The kinetic and physical basis of K(ATP) channel gating: toward a unified molecular understanding. *Biophys. J*. 78:2334–2348.
27. Inagaki, N., T. Gonoi, J. P. T. Clement, N. Namba, J. Inazawa, G. Gonzalez, L. Aguilar-Bryan, S. Seino, and J. Bryan. 1995. Reconstitution of IKATP: an inward rectifier subunit plus the sulfonylurea receptor. *Science*. 270:1166–1170.
28. Aguilar-Bryan, L., C. G. Nichols, S. W. Wechsler, J. P. T. Clement, A. E. R. Boyd, G. Gonzalez, H. Herrera-Sosa, K. Nguy, J. Bryan, and D. A. Nelson. 1995. Cloning of the beta cell high-affinity sulfonylurea receptor: a regulator of insulin secretion. *Science*. 268:423–426.
29. Sigworth, F. J. 1980. The variance of sodium current fluctuations at the node of Ranvier. *J. Physiol*. 307:97–129.
30. Neher, E., and C. F. Stevens. 1977. Conductance fluctuations and ionic pores in membranes. *Annu. Rev. Biophys. Bioeng*. 6:345–381.
31. Li, L., X. Geng, and P. Drain. 2002. Open state destabilization by ATP occupancy is mechanism speeding burst exit underlying KATP channel inhibition by ATP. *J. Gen. Physiol*. 119:105–116.
32. Trapp, S., P. Proks, S. J. Tucker, and F. M. Ashcroft. 1998. Molecular analysis of ATP-sensitive K channel gating and implications for channel inhibition by ATP. *J. Gen. Physiol*. 112:333–349.
33. Enkvetchakul, D., I. Jeliazkova, J. Bhattacharyya, and C. G. Nichols. 2007. Control of inward rectifier K channel activity by lipid tethering of cytoplasmic domains. *J. Gen. Physiol*. 130:329–334.
34. Shimomura, K., C. A. Girard, P. Proks, J. Nazim, J. D. Lippiat, F. Cerutti, R. Lorini, S. Ellard, A. T. Hattersely, F. Barbetti, and F. M. Ashcroft. 2006. Mutations at the same residue (R50) of Kir6.2 (KCNJ11) that cause neonatal diabetes produce different functional effects. *Diabetes*. 55:1705–1712.
35. Cukras, C. A., I. Jeliazkova, and C. G. Nichols. 2002. The role of NH(2)-terminal positive charges in the activity of inward rectifier K(ATP) channels. *J. Gen. Physiol*. 120:437–446.
36. Bhattacharyya, J., D. Enkvetchakul, D. Nelson, K. Markova, C. Cukras, I. Jeliazkova, and C. G. Nichols. 2003. Cloning and expression of bacterial Kirs. *Biophys. J*. 84:78a. (Abstr.)
37. Gopalakrishnan, K., G. Sowmiya, S. S. Sheik, and K. Sekar. 2007. Ramachandran plot on the web (2.0). *Protein Pept. Lett*. 14:669–671.
38. Haider, S., A. I. Tarasov, T. J. Craig, M. S. Sansom, and F. M. Ashcroft. 2007. Identification of the PIP_2-binding site on Kir6.2 by molecular modelling and functional analysis. *EMBO J*. 26: 3749–3759.
39. Schulze, D., T. Krauter, H. Fritzenschaft, M. Soom, and T. Baukrowitz. 2003. Phosphatidylinositol 4,5-bisphosphate (PIP_2) modulation of ATP and pH sensitivity in Kir channels. A tale of an active and a silent PIP_2 site in the N terminus. *J. Biol. Chem*. 278:10500–10505.
40. MacGregor, G. G., K. Dong, C. G. Vanoye, L. Tang, G. Giebisch, and S. C. Hebert. 2002. Nucleotides and phospholipids compete for binding to the C terminus of KATP channels. *Proc. Natl. Acad. Sci. USA*. 99:2726–2731.
41. Cukras, C. A., I. Jeliazkova, and C. G. Nichols. 2002. Structural and functional determinants of conserved lipid interaction domains of inward rectifying Kir6.2 channels. *J. Gen. Physiol*. 119:581–591.
42. Xie, L. H., S. A. John, B. Ribalet, and J. N. Weiss. 2007. Activation of inwardly rectifying potassium (Kir) channels by phosphatidylinositol-4,5-bisphosphate (PIP_2): interaction with other regulatory ligands. *Prog. Biophys. Mol. Biol*. 94:320–335.
43. Nichols, C. G. 2006. KATP channels as molecular sensors of cellular metabolism. *Nature*. 440:470–476.